

Nonequilibrium scaling explorations on a 2D Z(5)-symmetric model

Roberto da Silva*

*Instituto de Física, Universidade Federal do Rio Grande do Sul, Av. Bento Gonçalves,
9500 - CEP 91501-970, Porto Alegre, Rio Grande do Sul, Brazil*

Henrique A. Fernandes

*2 - Coordenação de Física, Universidade Federal de Goiás, Campus Jataí,
BR 364, km 192, 3800 - CEP 75801-615, Jataí, Goiás, Brazil*

J. R. Drugowich de Felício

*3 - Departamento de Física, Faculdade de Filosofia,
Ciências e Letras de Ribeirão Preto, Universidade de São Paulo,
Avenida Bandeirantes, 3900 - CEP 14040-901, Ribeirão Preto, São Paulo, Brazil*

We have investigated the dynamic critical behavior of the two-dimensional Z(5)-symmetric spin model by using short-time Monte Carlo (MC) simulations. We have obtained estimates of some critical points in its rich phase diagram and included, among the usual critical lines the study of first-order (weak) transition by looking into the order-disorder phase transition. Besides, we also investigated the soft-disorder phase transition by considering empiric methods. A study of the behavior of $\beta/\nu z$ along the self-dual critical line has been performed and special attention has been devoted to the critical bifurcation point, or FZ (Fateev-Zamolodchikov) point. Firstly, by using a refinement method and taking into account simulations out-of-equilibrium, we were able to localize parameters of this point. In a second part of our study, we turned our attention to the behavior of the model at the early stage of its time evolution in order to find the dynamic critical exponent z as well as the static critical exponents β and ν of the FZ-point on square lattices. The values of the static critical exponents and parameters are in good agreement with the exact results, and the dynamic critical exponent $z \approx 2.28$ very close of the 4-state Potts model ($z \approx 2.29$).

PACS numbers:

I. INTRODUCTION

In Statistical Mechanics, non-trivial models have been extensively studied after the exact solution of the two dimensional Ising model¹. A lot of authors have devoted an extensive use of several methods to describe the theory of magnetic systems by studying generalizations of such model, with more complex and richer phase diagrams. Among these models, one that deserves special attention is the Z(N) model whereas, differently of Ising model whose spin variable can assume only two values, each spin can assume N values and more than one coupling constant for $N > 4$. This leads to more delicate aspects with phase diagram that is not completely understood yet, even for example, for small values of N such as $N = 5$.

The two-dimensional Z(N) model contains several known systems as particular cases, for instance, the Ising ($N = 2$) and XY ($N = \infty$) models, as well as, the N -state scalar and vector Potts (clock) models, and the Ashkin-Teller model ($N = 4$). For $N \leq 4$, the phase diagram possesses a traditional second-order phase transition, and for $N = \infty$, it exhibits a Kosterlitz-Thouless type (KT) phase transition². But, for what N value does this last phase transition appear? Several works report that the KT phase transition appears at $N = 5^{3-7}$. The Z(5) model exhibits a rich phase diagram with first-order transitions, including the 5-state Potts point⁸, two

second-order transitions of the Ising type at Fateev-Zamolodchikov (FZ) integrability points⁵, and two lines of infinite-order transitions (dual to each other) of the KT type^{3,4,7,9-11} (see dashed lines in Fig. 1). Several works assert that the FZ points, henceforth named as “bifurcation point”, coincide with the points where the KT transitions are originated^{5,6,10,12,13}.

So, this interesting model and, in special the bifurcation points (for $N = 5$), deserves further explorations and non-equilibrium analysis can be an interesting alternative to obtain not only the static critical exponents but also the dynamical ones which have not yet been obtained in previous contributions. Moreover, this approach has proved to be efficient in determining the critical parameters of several models as shown in recent works (see for example the Refs.¹⁴⁻¹⁶).

In this paper, we present results from the study of the critical properties of the isotropic ferromagnetic two-dimensional spin model with Z(5) symmetry, hereafter denoted as Z(5) model, by using time-dependent MC simulations. As we are dealing with a symmetric model, the two bifurcation points are also symmetric and possess the same set of critical exponents. Hence, we concentrated in only one of them. Our contributions are divided in four parts as follows:

1. We estimated the critical parameters x_1 and x_2 of the bifurcation point⁵ by using a simple refinement method, in the context of time-dependent MC sim-

ulations which searches the best power law time decay of magnetization, as proposed in Ref.¹⁶;

2. We obtained the dynamic critical exponent z and the static critical exponents ν and β of the two independent order parameters of the model for the bifurcation point;
3. We explored several points on the self-dual line of the model by estimating the exponents of its two order parameters. We showed that the exponents are different along this line but respect a peculiar symmetry. However, for the particular point corresponding to the 5-state Potts model the critical exponents assume the same value;
4. We also explored and obtained some estimates of weak first-order points on the self-dual line and other second-order points on the soft-disorder transition line using an heuristic method, developed in this paper, that takes into account the second moment of the order parameters.

This article is organized as follows. In the next section we define the model and briefly discuss some peculiarities of its phase diagram. In Section III we present some finite size scaling relations in non-equilibrium spin systems theory and describe the power laws which are considered in this work to measure the required exponents and parameters. We also show how to simulate such behaviors via time-dependent Monte Carlo simulations. Our results are divided in two sections: In Section IV, we determined estimates of the phase transition points in the phase diagram by using a non-equilibrium approach and in Section V we specifically showed some estimates of critical exponents along the self-dual line with special attention to the FZ point. Finally, in Section VI we summarize and conclude our work.

II. THE MODEL AND ITS PHASE DIAGRAM

In this article we have studied the dynamic critical behavior of the Z(5) model by using short-time Monte Carlo simulations. The most general Hamiltonian of this model is given by

$$-\beta\mathcal{H} = \sum_{\langle i,j \rangle} k_1 \left[\cos \left(\frac{2\pi}{5} (n_i - n_j) \right) - 1 \right] + k_2 \left[\cos \left(\frac{4\pi}{5} (n_i - n_j) \right) - 1 \right], \quad (1)$$

where $\langle i, j \rangle$ indicates that the spin variables interact only with their nearest neighbors, i and j label the sites of a two-dimensional lattice of size $L \times L$, k_1 and k_2 are the two positive coupling constants, and $n_i = 0, 1, 2, 3, 4$ label the degrees of freedom of each site of the lattice.

In Fig. 1 (according to Ref.¹⁹) we can observe the phase diagram of this model translated to the suitable variables:

$$x_1 = \exp \left[\frac{\sqrt{5}(k_1 - k_2) - 5(k_1 + k_2)}{4} \right]$$

and

$$x_2 = \exp \left[\frac{\sqrt{5}(k_2 - k_1) - 5(k_1 + k_2)}{4} \right].$$

In the particular case $k_2 = k_1$ we recover the scalar 5-state Potts model and for $k_2 = 0$ the clock model. It is interesting to observe that 5-state Potts point corresponds to the meeting between the self-dual line defined by $x_1 + x_2 = (\sqrt{5} - 1)/2$ and the Potts physical line $x_1 = x_2$, this last one being a symmetry line of the diagram.

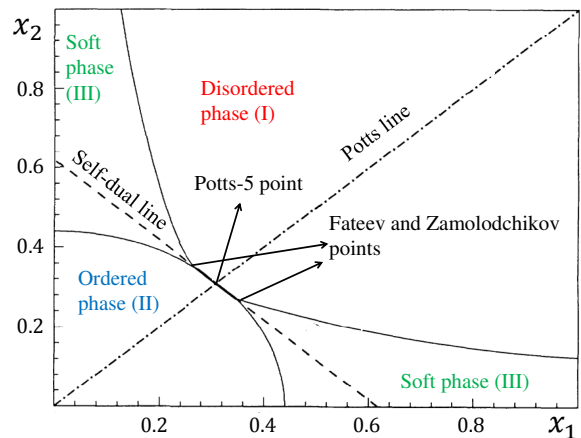


FIG. 1: (color online) Phase diagram of Z5-model according to the Ref.¹⁹. **Phase I**: Disordered phase, **II**: Ordered phase, and **III**: Soft phase. The 5-state Potts and FZ points are specifically indicated on the Self-dual line. The diagram is symmetric with respect to the Potts physical line.

In this work we are more concerned with the bifurcation point. Actually, as can be seen in Fig. 1 the model has two bifurcation points (FZ points) localized on the self-dual line. The phase transition line between the FZ points (which includes the Potts point) is of weak first order, and that on the right(left) of the rightmost(leftmost) FZ point, there are two continuous transition lines between ordered-soft and disordered-soft phases.

However the two bifurcation points are symmetric to each other and have the same set of critical exponents. For this reason, we took into account only one of them. The ratio of the coupling constants for the bifurcation point is given by $k_2/k_1 = (\sqrt{5} - 1)/2 \approx 0.618034$. Moreover, there are four order parameters but only two of them are independent ones²¹, namely

$$M_1 = \langle \delta_{n_i,1} - \delta_{n_i,2} \rangle \quad (2)$$

and

$$M_2 = \langle \delta_{n_i,1} - \delta_{n_i,3} \rangle, \quad (3)$$

where $\delta_{i,j}$ is the Kronecker's delta.

Since we established the main details of the model in order to calculate the critical parameters x_1 and x_2 , as well as the critical exponents z , β , and ν , we present in the next section the finite size scaling developed to describe non-equilibrium spin systems, the time-dependent power laws obtained from this approach, and some details about time-dependent MC simulations to be applied.

III. NON-EQUILIBRIUM DYNAMICS AND TIME-DEPENDENT MC SIMULATIONS

Until a few years ago, the numerical calculation of critical exponents was carried out only in equilibrium. Unfortunately, in this stage, the measurements of such exponents are very hard due to severe *critical slowing down* which takes place in the vicinity of the critical temperature. To circumvent this difficulty, some algorithms were proposed, for instance, the cluster algorithm^{22,23} that, although it is very efficient in the study of static properties, it violates the dynamic universality class of the specific local dynamics, such as the Model A.

Another way to avoid problems with the *critical slowing down* was proposed by Janssen, Schaub and Schmittmann²⁴ and Huse²⁵, both in 1989. They discovered using renormalization group techniques and numerical calculations, respectively, that there is universality and scaling behavior far from equilibrium. Since then, the so-called short-time regime has become an important method for the study of phase transitions and critical phenomena.

The dynamic scaling relation obtained by Janssen *et al.* for the k -th moment of the order parameter, extended to systems of finite size²⁶, is written as

$$\langle M^k \rangle(t, \tau, L, m_0) = b^{-k\beta/\nu} \langle M^k \rangle(b^{-z}t, b^{1/\nu}\tau, b^{-1}L, b^{x_0}m_0), \quad (4)$$

where t is the time evolution, b is an arbitrary spatial rescaling factor, $\tau = (T - T_c)/T_c$ is the reduced temperature and L is the linear size of the lattice. The exponents β and ν are the equilibrium critical exponents associated with the order parameter and the correlation length, and z is the dynamic exponent characterizing temporal correlations in equilibrium. Here, the operator $\langle \dots \rangle$ denotes averages over different configurations due to different possible time evolution from each initial condition of a given initial magnetization m_0 . For a large lattice size L and small initial magnetization m_0 at the critical temperature ($\tau = 0$), the Eq. (4) is governed by the new dynamic exponent θ , according to

$$\langle M \rangle_{m_0} \sim m_0 t^\theta, \quad (5)$$

if we choose the scaling factor $b = t^{1/z}$. This new exponent characterizes the so-called *critical initial slip*, the

anomalous behavior of the order parameter when the system is quenched to the critical temperature T_c .

Besides, a new critical exponent x_0 , which represents the anomalous dimension of the initial magnetization m_0 , is introduced to describe the dependence of the scaling behavior on the initial conditions. This exponent is related to θ as $x_0 = \theta z + \beta/\nu$. Actually the relaxation of spin systems is determined by two different behaviors, this initial slip and a second behavior corresponding to a power-law decay. This can be derived from the Eq. (4). After the scaling $b^{-1}L = 1$ at the critical temperature $T = T_c$, the first ($k = 1$) moment of the order parameter is $\langle M \rangle(t, L, m_0) = L^{-\beta/\nu} \langle M \rangle(L^{-z}t, L^{x_0}m_0)$.

Denoting $u = tL^{-z}$ and $w = L^{x_0}m_0$, one has $\langle M \rangle(u, w) = L^{-\beta/\nu} \langle M \rangle(L^{-z}t, L^{x_0}m_0)$. The derivative with respect to L is given by:

$$\begin{aligned} \partial_L \langle M \rangle &= (-\beta/\nu) L^{-\beta/\nu-1} \langle M \rangle(u, w) \\ &\quad + L^{-\beta/\nu} [\partial_u \langle M \rangle \partial_L u + \partial_w \langle M \rangle \partial_L w], \end{aligned}$$

where explicitly we have $\partial_L u = -ztL^{-z-1}$ and $\partial_L w = x_0 m_0 L^{x_0-1}$. In the limit $L \rightarrow \infty$, which implicates in $\partial_L \langle M \rangle \rightarrow 0$, one has $x_0 w \partial_w \langle M \rangle - zu \partial_u \langle M \rangle - \beta/\nu \langle M \rangle = 0$. The separability of the variables u and w , i.e., $\langle M \rangle(u, w) = M_u(u)M_w(w)$ leads to

$$x_0 w M'_w / M_w = \beta/\nu + zu M'_u / M_u,$$

where the prime means the derivative with respect to the argument. Since the left-hand side of this equation depends only on w and the right-hand side depends only on u , both sides must be equal to a constant c . Thus, $M_u(u) = u^{c/z} - \beta/(\nu z)$ and $M_w(w) = w^{c/x_0}$, resulting in $\langle M \rangle(u, w) = m_0^{c/x_0} L^{\beta/\nu} t^{(c-\beta/\nu)/z}$. Returning to the original variables, one has $\langle M \rangle(t, L, m_0) = m_0^{c/x_0} t^{(c-\beta/\nu)/z}$.

On one hand, by choosing $c = x_0$ at criticality ($\tau = 0$), one obtains $\langle M \rangle_{m_0} \sim m_0 t^\theta$, where $\theta = (x_0 - \beta/\nu)/z$ that corresponds to a regime of small initial magnetization soon after a finite time scaling $b = t^{1/z}$ in Eq. 4. This leads to $\langle M \rangle(t, m_0) = t^{-\beta/(\nu z)} \langle M \rangle(1, t^{x_0/z} m_0)$. By calling $x = t^{x_0/z} m_0$, an expansion of the averaged magnetization around $x = 0$ results in $\langle M \rangle(1, x) = \langle M \rangle(1, 0) + \partial_x \langle M \rangle|_{x=0} x + \mathcal{O}(x^2)$. By construction $\langle M \rangle(1, 0) = 0$ and, since $u = t^{x_0/z} m_0 \ll 1$, we can discard quadratic terms resulting in $\langle M \rangle_{m_0} \sim m_0 t^\theta$. This anomalous behavior of initial magnetization is valid only for a characteristic time scale $t_{\max} \sim m_0^{-z/x_0}$.

On the other hand, the choice $c = 0$ corresponds to the case where the system does not depend on the initial trace and $m_0 = 1$ leads to simple power law:

$$\langle M \rangle_{m_0=1} \sim t^{-\beta/(\nu z)} \quad (6)$$

that similarly corresponds to the decay of magnetization (for $t > t_{\max}$) of a system previously evolved from an initial small magnetization (m_0), and that had its magnetization increased according to Eq. 5 up to a peak.

For $m_0 = 0$, it is not difficult to show that the second moment of the magnetization is given by

$$\langle M^2 \rangle_{m_0=0} \sim t^\varsigma, \quad (7)$$

with $\varsigma = (d - 2\beta/\nu)/z$, where d is the dimension of the system. By using short-time MC simulations, where lattices are suitably prepared with a fixed initial magnetization, many authors have obtained the dynamic exponent z as well as the static ones β and ν , for many different models (see, for example, two good reviews can be found in Refs.^{27, 28}).

In order to estimate independently the critical exponents, we can, firstly, determine z by using a power law that mixes initial conditions²⁹ as follows

$$F_2(t) = \frac{\langle M^2 \rangle_{m_0=0}}{\langle M \rangle_{m_0=1}^2} \sim t^\xi, \quad (8)$$

where $\xi = d/z$. With the estimate of ξ , denoted here by $\hat{\xi}$, we are able to obtain an estimate of z (given by $\hat{z} = d/\hat{\xi}$) independent of other parameters. In order to obtain ν , we use an alternative power law. When considering $m_0 = 1$ in Eq. 4, one can see that there is no dependence on the initial configurations. Therefore, when $L \rightarrow \infty$, one can $\langle M \rangle(t, \tau) = b^{-k\beta/\nu} \langle M \rangle(b^{-z}t, b^{1/\nu}\tau)$. By scaling $b^{-z}t = 1$, we have $\langle M \rangle(t, \tau) = t^{-\beta/(\nu z)} f(t^{1/(\nu z)}\tau)$ where $f(x) = \langle M \rangle(1, x)$ and so $\partial \ln \langle M \rangle(t, \tau) / \partial \tau = \frac{1}{\langle M \rangle} \frac{\partial}{\partial \tau} \langle M \rangle = t^{1/(\nu z)} f(t^{1/(\nu z)}\tau)$. Therefore we have

$$D(t) = \left. \frac{\partial \ln \langle M \rangle}{\partial \tau} \right|_{\tau=0} = f_0 \cdot t^{1/(\nu z)} \sim t^\phi \quad (9)$$

where $f_0 = f(0)$ is a constant and $\phi = 1/(\nu z)$. Since we have already obtained the exponent z , we are able to obtain ν . With these two exponents in hand, we can obtain β by estimating the exponent $\mu = \beta/(\nu z)$ from Eq. 6.

In order to simulate numerically the theoretical moments of the magnetization of the spin systems as functions of time, we used a local dynamic evolution of the spins which are updated by the heat-bath algorithm. In our simulations we used two different initial states: to obtain the power laws giving by the Eqs. 6 and 9, we used the initial ordered state, i.e., $m_0 = 1$ ($\sigma_i \equiv 1$, $i = 1, \dots, N = L^d$). On the other hand, when considering the Eq. 7 we used a initial state with $m_0 = 0$, i.e., the spins of each site were chosen at random on the sites but keeping the same proportion - $L^d/5$ spins of each type: $\sigma_i = 0, 1, 2, 3, 4$. Here it is important to mention that $m_0 = 0$ for any order parameter proposed in our analysis [Eqs. 2 and 3].

In the context of time-dependent MC simulations, the magnetization ($k = 1$) and its higher moments ($k > 1$) have statistical estimators for the theoretical moments (4) given by

$$\langle M^k \rangle(t) = \frac{1}{N_{run} L^d} \sum_{j=1}^{N_{run}} \left(\sum_{i=1}^{L^d} \sigma_{i,j}(t) \right)^k,$$

where $\sigma_{i,j}(t)$ denotes the i -th spin variable on the lattice at t -th MC step of the j -th run. Here N_{run} denotes the number of different repetitions (runs) or different time series used to compute the averages.

IV. RESULTS I: EXPLORING THE PHASE DIAGRAM VIA NON-EQUILIBRIUM MC SIMULATIONS

Our initial plan was to study the phase transition points of the Z(5) model via time-dependent MC simulations by estimating the best x_2 given as input the parameter x_1 according to the phase diagram (see Fig. 1). We performed this task for several points in this diagram and the analysis was carried out by using an approach developed in¹⁶ in the context of generalized statistics. This tool had also been applied successfully to study multicritical points, for example, tricritical points^{15,30} and Lifshitz point of the ANNNI model¹⁴.

Since at criticality is expected that the order parameter obeys the power law behavior of Eq. 6, we fixed the value of x_1 and changed the value of x_2 according to a resolution Δx_2 . Then, we calculated the known coefficient of determination¹⁷ that, for our case, is given by:

$$r = \frac{\sum_{t=1}^{N_{MC}} (\overline{\ln \langle M \rangle} - a - b \ln t)^2}{\sum_{t=1}^{N_{MC}} (\ln \langle M \rangle - \ln \langle M \rangle(t))^2}, \quad (10)$$

with $\overline{\ln \langle M \rangle} = (1/N_{MC}) \sum_{t=1}^{N_{MC}} \ln \langle M \rangle(t)$, for each value $x_2 = x_2^{(\min)} + i\Delta x_2$, with $i = 1, \dots, n$, where $n = \left\lfloor (x_2^{(\max)} - x_2^{(\min)}) / \Delta x_2 \right\rfloor$, and the critical value corresponds to $x_2^{(opt)} = \arg \max_{x_2 \in [x_2^{(\min)}, x_2^{(\max)}]} \{r\}$. The coefficient r has a very simple explanation: it measures the ratio: (expected variation)/(total variation). The bigger the r , the better the linear fit in log-scale, and therefore, the better the power law which corresponds to the critical parameter except for an error $O(\Delta x_2)$.

As we are dealing with a rich phase diagram, a careful analysis of the order of the phase transition is necessary, mainly when taking into account first-order “critical” points. As pointed out earlier, the phase diagram of the Z(5) model possesses two second-order phase transition points which coincide with the FZ integrability points, as well as two lines of infinite-order transition (dual to each other) also known as self-dual lines. The phase transitions of the points on these lines which extend from the 5-state Potts point to the FZ points are expected to be of first-order. Although it is not expected a power law behavior of the order parameter at strong first-order points, it is possible to obtain this behavior for weak first-order ones, whereas for $k > k_c$ a disorder metastable state vanishes at a certain k^* and, for $k < k_c$, there is an ordered metastable state which disappears at k^{**} . Both parameter values look like critical points if the system remains

in the disordered or ordered metastable states, and so in both points a power law behavior must be observed as studied by Schulke and Zheng¹⁸ through the analysis of the weakness of first-order phase transition in the q -state Potts model. In that case a good estimate for k_c would be $(k^* + k^{**})/2$. For the 5-state Potts model, for example, the difference between the pseudo critical points k^* or k^{**} and k_c is in the fourth decimal digit. Moreover, the difference between power laws obtained from the pseudo critical points and k_c is observed for $t \sim 1000$ MC steps.

Since the self-dual line of the Z(5) model is analytically described by $x_2 = \frac{(\sqrt{5}-1)}{2} - x_1$ and the points extending from $x_1 = (\sqrt{5}-1)/4 \approx 0.30901\dots$ to (but not including) the FZ point (which corresponds to $x_1 \approx 0.3473834\dots$) are points of weak first-order transition, we determined the corresponding x_2 via method previously described. In this case, by looking into the difference between x_2 (exact) and x_2 (simulation), it was possible to have a measure of weakness of the considered points.

In TABLE I, third column, we show our results for x_2 (x_2^{opt}) for five points along the self-dual line that whose transitions are expected to be of first-order, as well as for the FZ point (sixth line). In order to obtain these results, we used resolution of $\Delta x_2 = 0.002$ and applied a simple algorithm that makes a process of refinement of the parameter in order to localize the best x_2 along the simulations. These values must be compared to the exact predictions of the self-dual line (second column). It is important to notice that the columns 4, 5, and 6 represent, respectively, the values of r obtained for the fits with respective values of x_2 : $x_2^{opt} - \Delta x_2$, x_2^{opt} , and $x_2^{opt} + \Delta x_2$. For instance, we observe that, for the Potts point $r(x_2^{opt} - \Delta x_2) = 0.994251$, $r(x_2^{opt}) = 0.999605$ and $r(x_2^{opt} + \Delta x_2) = 0.999557$. From that, we applied a second refinement for the interval $[x_2^{opt} - \Delta x_2, x_2^{opt} + \Delta x_2]$ by using $\Delta x_2 = 10^{-4}$ and we found 0.3094(1) (seventh column). When compared to the exact value 0.30901... we observed an error only in the fourth decimal place which is reasonable according to lattice used in our MC simulations for this optimization, $L = 160$.

Now, since we analyzed the first-order (weak) transition up to the bifurcation point, we turned our attention to points after it via time dependent MC simulations. According to these phase diagram (Fig. 1), after the bifurcation point, $x_1 > 0.3473834\dots$, there are two second-order lines separating the ordered and disordered phases and the soft one.

For example, by applying our refinement process for $x_1 = 0.42$, the method produces a clear point where r is maximum $x_2^{opt} = 0.198(2)$ (see plot (a) in Fig. 2). This value is in complete agreement with the exact value of the self-dual line, $x_2 = \frac{(\sqrt{5}-1)}{2} - 0.42 = 0.19803\dots$. However, it is important to notice that we did not find the two points which we would expect by looking into the phase diagram corresponding to the two critical lines. In order to better exploit such specificities, we simulated our method for two other inputs: $x_1 = 0.44$ and $x_1 =$

0.46, the first one corresponds to the end of soft-order transition and the second one was chosen because there is no ordered phase at this point (see plots (b) and (c) in Fig. 2).

In those cases we can clearly see that there is no a unique point where r assumes a maximum value. Finally in the same Fig. 2 (plot (d)) we show the behavior of this same coefficient for some important points just for an appropriated comparison: the 5-state Potts model (weak first-order transition point), $x_1 = 0.4$ (crossing two second-order lines), $x_1 = 0.5$, and specially the FZ point whose critical exponents are estimated in this paper. Now we would like to consider alternatives to determine (localize) points after the bifurcation point that are localized on the soft-disorder transition line. From now on, we will be much more empirical in our techniques. As we reported above, our optimization method captures the points on the self-dual line but the points corresponding to soft-disorder and soft-order transitions seems to be neglected by the method and this deserves a better investigation.

Since we used the power laws for ordered initial spin systems, this can be the reason whereas such transitions are not order-disorder-like. In order to localize such points we prepared a second algorithm similar to the previous method. However, instead of optimizing the Eq. 6, by performing several time-dependent MC simulations starting from $m_0 = 1$, we monitored simulations starting from $m_0 = M_1(0) = 0$ and, in this case, we expected that the second moment of the order parameter has the power law given by Eq. 7 (see³²). Moreover, we also monitored the value of ς whereas it can be estimated, even without significance, when the coefficient of determination is not satisfactory.

Fig. 3 shows the behavior of the coefficient of determination when one takes into account the power laws for $\langle M \rangle_{m_0=1}$ and $\langle M^2 \rangle_{m_0=0}$ along with the numerical estimates of ς , for two input values: $x_1 = 0.36$ (plot (a)) and $x_1 = 0.46$ (plot (b)). We can see that determination for $\langle M^2 \rangle_{m_0=0}$ for both values decreases abruptly for a value of x_2 followed by a subsequent abrupt increase. Such behavior was found for other several studied points ranging from the 5-state Potts model to $x_1 = 0.6$. We also can see that the peak of the curves of coefficient of determination correspond to the points where the numerical estimates of ς change their signal. For instance, for $x_1 = 0.36$, we found a clear maximum of the determination coefficient for $x_2 = 0.258(2)$ when we consider fits for $\langle M \rangle$ (Eq. 6). On the other hand, when one considers fits for $\langle M^2 \rangle$ (Eq. 7) the value of x_2 at the peak of the determination coefficient ($x_2 = 0.278(2)$) does not coincide with the previous one.

In order to establish some relationships between the estimates of the points where there is an abrupt decreasing of coefficient r for $\langle M^2 \rangle$ and values of the soft-disorder transition, we decided to digitize the phase diagram of the model (Fig. 1, Ref.¹⁹) in order to localize (by using a pointer on the bitmap figure) and compare some points

x_1	$x_2(\text{exact})$	$x_2^{\text{opt}}(\text{simulation})$	$r(x_2^{\text{opt}} - \Delta x_2)$	$r(x_2^{\text{opt}})$	$r(x_2^{\text{opt}} + \Delta x_2)$	$(x_2^{\text{opt}})^{(2)}$
Potts 5	0.30901...	0.308(2)	0.994251	0.999605	0.999557	0.3094(1)
0.31	0.30803...	0.308(2)	0.997386	0.999514	0.998977	0.3083(1)
0.32	0.29803...	0.298(2)	0.997535	0.999696	0.997920	0.2979(1)
0.33	0.28803...	0.288(2)	0.998707	0.999715	0.998626	0.2873(1)
0.34	0.27803...	0.278(2)	0.998385	0.999572	0.998690	0.2781(1)
FZ	0.27065...	0.270(2)	0.999401	0.999701	0.999168	0.2702(1)

TABLE I: Analysis of the weak first-order transitions until the critical point FZ

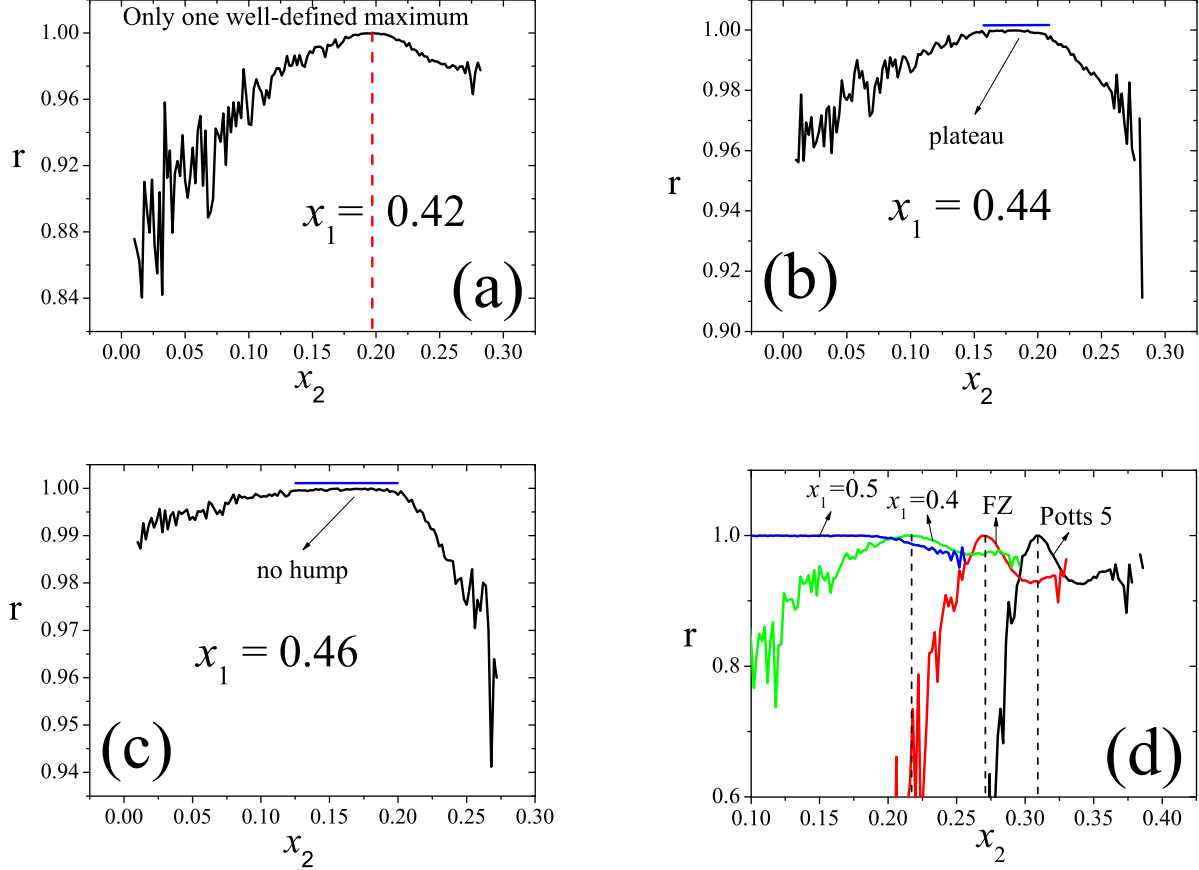


FIG. 2: (color online) **Plot (a)**: Refinement process for the input $x_1 = 0.42$. A clear point where r is maximum is found. The **plots (b) and (c)** show, respectively, the refinement for $x_1 = 0.44$ and $x_1 = 0.46$. In these cases there is no a notorious optimization point since $x_1 = 0.44$ is the last point where we expect to find an order-disorder transition. **Plot (d)**: The refinement process for the FZ point and for other 3 additional points: 5-state Potts point, $x_1 = 0.4$, and $x_1 = 0.5$.

of soft-disorder phase transition to the values obtained in our simulations.

We can observe that after $x_1 = 0.40$ (see TABLE II) there is an excellent agreement between unofficial estimates (Ref.¹⁹) and our empirical method (EM). It is important to mention that before $x_1 = 0.44$ our method for optimization of the power law for $\langle M \rangle_{m_0=1}$ has already localized very well the considered points on the self-dual transition line. So from this analysis we have

two important conclusions:

1. By taking into account points with $(\sqrt{5} - 1)/4 < x_1 < 0.44$, we are able to estimate the best values of x_2 which corresponds to the self-dual line by optimizing the Eq. 6.
2. For $x_1 \geq 0.40$ we estimated some values of x_2 through the Eq. 7 by using an empirical approach and analyzed the soft-disorder transition, the only

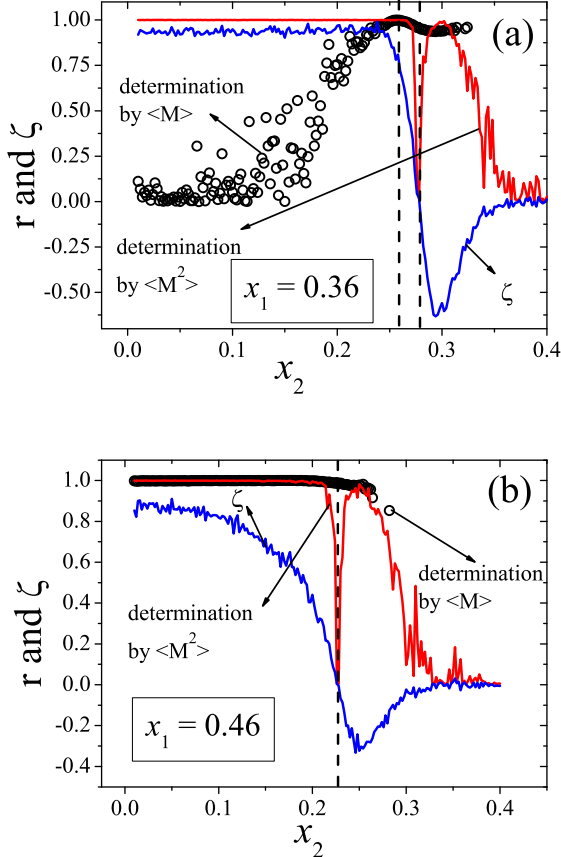


FIG. 3: (color online) Coefficient of determination for the two different power law fits: $\langle M \rangle_{m_0=1} \sim t^{-\beta/\nu z}$ and $\langle M^2 \rangle_{m_0=0} \sim t^{(d-2\beta/\nu)z}$, and evaluation of the coefficient $\zeta = (d - 2\beta/\nu)z$ for the different values of x_2 considering as input: $x_1 = 0.36$ (plot a) and $x_1 = 0.46$ (plot b)

transition above the self-dual line, in this region predicted by the phase diagram (see¹⁹).

Finally, it is important to mention a technical detail in our simulations. Here, our initial condition for obtaining $m_0 = 0$ for $\langle M^2 \rangle$ was built only with spins related to the first order parameter (Eq. 2), i.e., $n_i = 1$ or 2. This case does not correspond to the correct critical values of β and ν , whereas the correct way to vanish the initial configuration is to put $n_i = 0, 1, 2, 3, 4$ in the proportion of 1/5 for each one, as used in this paper to compute the critical exponents. However, when considering the empirical method presented above this initial condition ($n_i = 1$ or 2) brings a change of signal of ζ which was not observed when considering the initial natural condition (proportion of 1/5).

x_1	$x_2(\text{Ref.}^{19})$	$x_2(\text{EM})$
FZ	0.270	0.288(2)
0.36	0.264	0.278(2)
0.40	0.252	0.250(2)
0.44	0.230	0.232(2)
0.48	0.220	0.220(2)
0.52	0.209	0.208(2)

TABLE II: Values of x_2 for several points (first column) obtained through two methods. The second column presents the estimates extracted by the digitalization of the Fig. 1 in Ref.¹⁹ and the third column shows the values obtained by an alternative empirical method (EM)

V. RESULTS II: ESTIMATING THE CRITICAL EXPONENTS (STATIC AND DYNAMIC ONES) OF THE BIFURCATION POINT

Now we explored the critical exponents of Z(5) model with special attention to the bifurcation point. Before showing the estimates for this point, we presented some estimates of the exponent $\mu_i = -\beta/\nu z$ from Eq. 6, with $i = 1$ or 2, along self-dual line by using the two order parameters M_i (Eqs. 2 and 3). Our main idea here is to study the symmetry between these two order parameters via non-equilibrium MC simulations and to explore if there is some pair (x_1, x_2) for which $\mu_1 = \mu_2$. It is important to mention that μ is a sort of effective exponent since it was used to analyze first weak and second order points.

A. Exploring the self-dual line

We prepared an algorithm that measures μ for each (x_1, x_2) pair in the self-dual line: $x_2 = (\sqrt{5} - 1)/2 - x_1$ and performed time-dependent MC simulation to obtain averages of the order parameter (Eq. 2 and 3) and, consequently, the exponents μ_1 and μ_2 from the power law decay (Eq. 6). For these simulations, we considered x_1 ranging from $x_1^{(\min)} = 0.2$ to $x_1^{(\max)} = 0.4$, with $\Delta x_1 = 5 \cdot 10^{-3}$. For each input pair (x_1, x_2) we used $N_{run} = 1200$ runs, $N_{MC} = 150$ and $L = 160$ (enough after a fast finite size scaling study as shown in the next subsection).

In Fig. 4 we show the behavior of μ_1 and μ_2 as function of x_1 . We can observe that the curves meet each other at the point $x_1 = 0.310(5)$ which corresponds to the numerical estimate of the 5-state Potts point as well as to the symmetry found in the phase diagram presented in Fig. 1. Undoubtedly, this is another interesting finding obtained when using non-equilibrium MC simulations. It is important to say that we obtained a goodness-of-fit (see for example²⁰) above 0.99 for all considered points showing that all estimates were obtained with robust power law decays. After these preliminary explorations of the

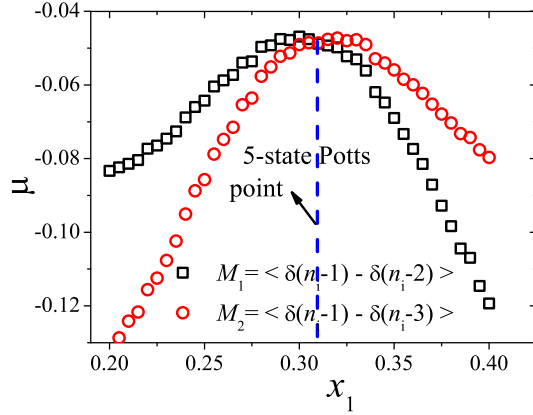


FIG. 4: (color online) Estimates of the exponent $\mu = -\beta/\nu z$ (a sort of effective exponent) along self-dual line. We can observe that curves assume the same value in $x_1 = 0.310(5)$ which corresponds to the 5-state Potts point.

self-dual line and its symmetry via non-equilibrium MC simulations we explored the numerical estimates of the critical exponents at the FZ point.

B. The exponents z , ν and β of the FZ point

Initially we performed simulations to obtain F_2 as function of t . In order to verify the finite-size effects, we have used lattice of linear sizes, $L = 10, 20, 40, 80, 160$, and 240 . In Fig. 5 we can observe robust power laws for the time evolution of the ratio F_2 . As can be seen in the figure, the power law behavior of the first order parameter, M_1 , is showed as point while the second one, M_2 , is represented by lines. Then, it is possible to notice in this figure that both order parameters share the same exponent z .

In our experiments we used $N_{MC} = 150$ MC steps and calculated the exponents for different time windows of size $\Delta N = 10$ MC steps with respective goodness of fit q . In TABLE III (3rd column) we show the different values obtained for z . All intervals presented excellent goodness of fit (6rd column), with $q_z > 0.73$.

Similarly, the plots in Figs. 6 and 7 show the time evolution of $D(t)$ and $M(t)$, for the two different order parameters. Here, $D(t)$ was numerically estimated according to

$$D(t) \approx \frac{1}{2\delta} \ln \left[\frac{\langle M \rangle(t, T_c + \delta)}{\langle M \rangle(t, T_c - \delta)} \right]$$

where $\langle M \rangle(t, T_c \pm \delta)$ means the magnetizations above (below) critical temperature of a quantity δ , starting from ordered initial state. Since our parameters are $k_1 = J_1/k_B T$ and $k_2 = J_2/k_B T$ a perturbation of δ in

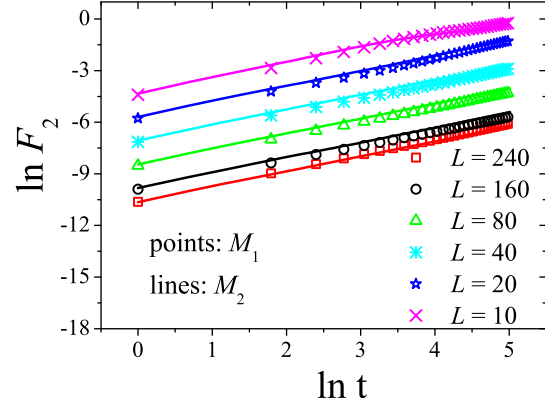


FIG. 5: (color online) Time evolution of F_2 in a ln-ln plot. The points correspond to the behavior of order parameter M_1 while lines correspond to the order parameter M_2 .

Interval	$\phi = 1/\nu z$	z	$\mu = \beta/\nu z$	$q_{1/\nu z}$	q_z	$q_{\beta/\nu z}$
[30, 40]	0.666(6)	2.38(3)	0.0641(2)	0.994	0.998	0.989
[40, 50]	0.649(5)	2.43(5)	0.0650(4)	0.998	1.000	1.000
[50, 60]	0.667(6)	2.34(6)	0.0650(7)	0.999	1.000	1.000
[60, 70]	0.659(6)	2.40(5)	0.065(1)	0.995	1.000	1.000
[70, 80]	0.64(1)	2.28(6)	0.066(1)	1.000	1.000	1.000
[80, 90]	0.66(2)	2.24(6)	0.066(1)	1.000	1.000	1.000
[90, 100]	0.65(2)	2.34(6)	0.067(2)	0.998	1.000	1.000
[100, 110]	0.63(2)	2.35(5)	0.065(1)	1.000	0.993	1.000
[110, 120]	0.66(1)	2.32(3)	0.067(2)	0.999	0.917	1.000
[120, 130]	0.64(2)	2.32(4)	0.066(3)	1.000	0.968	1.000
[130, 140]	0.68(2)	2.33(5)	0.066(2)	1.000	0.986	0.999
[140, 150]	0.66(1)	2.29(4)	0.067(3)	0.999	0.737	1.000

TABLE III: Estimates of exponents for different time windows by using the order parameter M_1

T corresponds to $k'_1 = J_1/k_B(T \pm \delta) = k_1/(1 \pm \delta')$ and $k'_2 = k_2/(1 \pm \delta')$, where $\delta' = \delta/T$.

In TABLE III we also present our results for ϕ and μ exactly as previously reported for z . We can observe again good fits in all time windows. All the analysis and estimates presented above for M_1 were also performed for the second order parameter, M_2 . However, for economy they were not reported here whereas a compilation of our main estimates, including M_1 and M_2 are presented in IV. The results from 2nd to 7th columns are estimated by using the regular method to obtain the error bars in the context of short time critical MC simulations, via error propagation (see first part of the appendix).

In this table, the term "best" means the best value found which reproduces the most similar conjectured values for the static exponents ν and β (10th and 11th columns, respectively). The term "prop" refers to uncertainty which was calculated by error propagation.

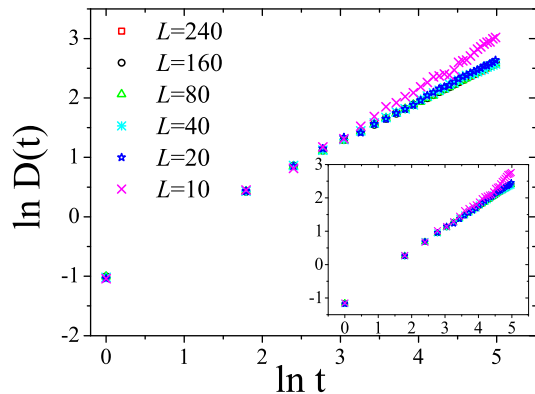


FIG. 6: (color online) Time evolution of $D(t)$ in a \ln - \ln plot for order parameter M_1 . The inset plot represents the same time evolution for the order parameter M_2 . Just for $L = 10$ we can observe a visual reasonable deviation of the power law behavior.

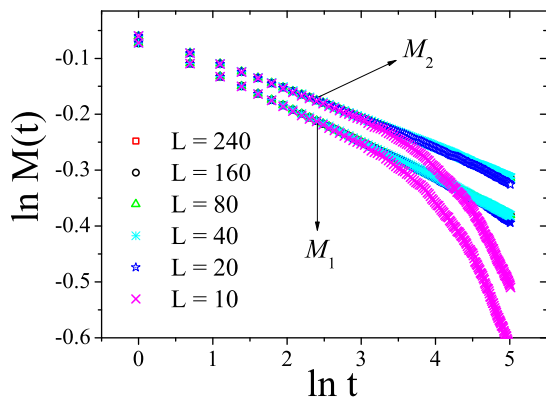


FIG. 7: (color online) Decay of the magnetization starting from an ordered initial state. The branches for each order parameter, M_1 and M_2 , are indicated in plot. The difference between the slopes indicates the difference between critical exponents β_1 and β_2 .

The term "aver" means the average of exponents performed from larger time windows taking the estimates from [70, 80] up to [140, 150].

We used an alternative method to obtain better estimates, considering bootstrap re-sampling method for the uncertainty calculation (see second part of the appendix for detailed description). The idea is to overcome possible statistical correlation among the exponents. The results are presented in 8th and 9th columns. Our estimates by using bootstrap re-sampling (boot in table IV) corroborate the exact values for ν and β .

First of all, it is important to mention that we ob-

tained estimates of exponent z for both order parameters which, to our knowledge, have never been calculated. We can see values greater than estimates for the Ising model for example ($2.14 \lesssim z \lesssim 2.16$) and 3-state Potts model ($z \approx 2.19$)²⁹, but similar to results obtained for the 4-state Potts model ($z \approx 2.29$)³¹. The exponents z , for both order parameters, are in complete agreement according to error bars. By using error propagation, our estimates for β ($\beta^{(prop)}$) over any criteria are rigorously according to conjecture value $\beta = 0.08$ for the order parameter M_2 . On the contrary, although we have reasonable results for the order parameter M_1 , $\beta_{best}^{(prop)} = 0.107(4)$ and $\beta_{aver}^{(prop)} = 0.105(3)$, the error bars are not enough to cover the conjectured value $\beta = 0.12$.

Alternatively, with the procedure described in the second part of the appendix that combines bootstrap and selection, we have as best estimate $\beta_{best}^{(boot)} = 0.119(3)$ satisfying the conjecture.

We finally found $\nu_{best}^{(prop)} = 0.70(2)$ and $0.70(3)$ for M_1 and M_2 respectively, which corroborates the conjecture $\nu = 0.7$.

VI. DISCUSSION AND CONCLUSIONS

In this paper we studied the phase diagram of $Z(5)$ model through non-equilibrium finite size scaling study in the context of time-dependent MC simulations. We determined some critical values and weak first-order transition values along the self-dual line with special attention to FZ point that, to our knowledge, have never been analyzed using this approach. We also determined some transition points along the soft-disorder transition line by using a non-conventional way that looks for an abrupt "depression" on the second moment of the order parameter as function of time. Moreover, we calculated the exponent $\mu = \beta/\nu z$ for several points on the self-dual line of the model for the two order parameters and we showed that these exponents are equal for the two order parameters only for the point correspondent to the 5-state Potts point.

VII. APPENDIX

In this section we present our methods to estimate uncertainties. In this paper we used two approaches: (1) error propagation: generally used in short time dynamics literature and (2) alternative error analysis by using bootstrap estimate.

A. Error propagation

In this paper, we used $N_{run} = 4 \times 10^5$ runs for the computation of averaged time series of the second moment of the order parameters, Eq. 7, in which require disordered

OP	$\nu_{best}^{(prop)}$	$\nu_{aver}^{(prop)}$	$\beta_{best}^{(prop)}$	$\beta_{aver}^{(prop)}$	$z_{best}^{(prop)}$	$z_{aver}^{(prop)}$	$\nu_{best}^{(boot)}$	$\beta_{best}^{(boot)}$	ν_{exact}	β_{exact}
M_1	0.70(2)	0.66(1)	0.107(4)	0.105(3)	2.28(6)	2.31(1)	0.70(3)	0.119(3)	0.7	0.12
M_2	0.70(3)	0.68(1)	0.080(1)	0.081(1)	2.28(8)	2.26(1)	0.70(4)	0.080(2)	0.7	0.08

TABLE IV: Final estimates of critical exponents for both order parameters (OP). Here the "best" denotes the value used to obtain the static critical exponents more similar to literature. "aver" denotes the value found by performing an average over time windows as shown in table III for the order parameter M_1

initial configurations, and $N_{run} = 10^4$ runs for experiments that demand ordered initial configurations, such as those which take into account the power laws given by the Eqs. 6, 8 and 9.

The error bars were obtained from $N_b = 5$ different bins. Our results, presented in the following plots, correspond to more refined estimates $\overline{M^k(t)} = (1/N_b) \sum_{i=1}^{N_b} \langle M^k(t) \rangle^{(i)}$ and the error bars (standard deviation of average) were estimated as $\sigma/\sqrt{N_b} = \left(\frac{1}{N_b(N_b-1)} \sum_{i=1}^{N_b} \left[\langle M^k(t) \rangle^{(i)} - \overline{M^k(t)} \right]^2 \right)^{1/2}$, where $\langle M^k(t) \rangle^{(i)}$ denotes the average of k -th moment of magnetization of the i -th bin.

The exponent z was estimated from Eq. 8 as $\hat{z} = 2/\hat{\xi}$ (by setting $d = 2$) and its error, σ_z , was obtained through the equation $\sigma_z = (2/\hat{\xi}^2)\sigma_{\xi}$, where σ_{ξ} is the error obtained from the power law fit. With the estimate of z and its respective uncertainty in hand, we were able to obtain an estimate of ν ($\hat{\nu}$) through the fitting of the Eq. 9, i.e., $\hat{\nu} = \hat{\phi}^{-1}\hat{z}^{-1}$, with its respective uncertainty:

$$\sigma_{\nu} = \left[\hat{\phi}^{-2}\hat{z}^{-4}\sigma_z^2 + \hat{\phi}^{-4}\hat{z}^{-2}\sigma_{\hat{\phi}}^2 \right]^{1/2}.$$

Now, we can estimate β . Whereas we have in hand an estimate of $\hat{\phi}$, we can estimate β , where by fitting the Eq. 6 $\hat{\beta} = \hat{\mu}/\hat{\phi}$, with respective uncertainty

$$\sigma_{\beta} = \left[\hat{\phi}^{-2}\sigma_{\mu}^2 + \hat{\phi}^{-4}\hat{\mu}^2\sigma_{\hat{\phi}}^2 \right]^{1/2}.$$

B. Alternative approach with Bootstrap estimates

Now we describe an alternative analysis for estimating exponents with uncertainties calculated by the bootstrap method. Let us start by the independent exponent z . So, instead of determining this exponent by combining 5 seeds which corresponds to 5 different time series: $t \times F_2(t)$, and obtaining the error bars over these 5 seeds for each point of averaged time series, we used a different procedure. Since we have 5 seeds for $\langle M \rangle_{m_0=1}$ and 5 seeds for $\langle M^2 \rangle_{m_0=0}$ we can obtain $N_{bin} = 25$ different time series $t \times F_2(t)$ by crossing the seeds. So, we obtain $N_{sample}^{(boot)}$ different re-sampled data set obtained with replacement. For each data set, each time series

$[t \times F_2(t)]_i$ corresponds to a specific bin $i = 1, \dots, N_{bin}$, and an exponent z_i is calculated. Then, for every re-sampled data set would be for example: $sample_1 = (z_1^{(1)}, z_2^{(1)}, \dots, z_{25}^{(1)})$, $sample_2 = (z_1^{(2)}, z_2^{(2)}, \dots, z_{25}^{(2)})$, ..., $sample_{N_{sample}} = (z_1^{(N_{sample}^{(boot)})}, z_2^{(N_{sample}^{(boot)})}, \dots, z_{25}^{(N_{sample}^{(boot)})})$. So for every re-sampled data we calculate $\langle z \rangle_{(i)} = (z_1^{(i)} + \dots + z_{25}^{(i)})/N_{bin}$, and with a sampling distribution of $\langle z \rangle_{(i)}$ we calculate $\langle z \rangle = (1/N_{sample}^{(boot)}) \sum_{i=1}^{N_{sample}^{(boot)}} \langle z \rangle_{(i)}$. The standard deviation of the sampling is given by $\sigma_z = \sqrt{(N_{sample}^{(boot)} - 1)^{-1} \sum_{i=1}^{N_{sample}^{(boot)}} (\langle z \rangle_{(i)} - \langle z \rangle)^2}$ which is a standard error of the mean (this is the more important point).

Since we obtained previously an estimate of z , we used it as input and we calculated $\nu^{(boot)}$ by using time series $t \times \frac{1}{2\delta} \ln \left[\frac{\langle M \rangle_{m_0=1}(t, k_c + \delta)}{\langle M \rangle_{m_0=1}(t, k_c - \delta)} \right]$. We also crossed the seeds to obtain $N_{bin} = 25$ bins and for each bin, a linear fit is performed producing $\phi_i \Rightarrow \nu_i = 1/(\phi_i \cdot z)$. We repeat the re-sampling procedure in order to obtain: $\sigma_{\nu} = \sqrt{(N_{sample}^{(boot)} - 1)^{-1} \sum_{i=1}^{N_{sample}^{(boot)}} (\langle \nu \rangle_{(i)} - \langle \nu \rangle)^2}$. Finally, since we have estimates for z and ν we repeat the procedures to obtain the error estimate of β : a) Linear fits produce $\mu_i \Rightarrow \beta_i = z \cdot \nu \cdot \mu_i$, $i = 1, \dots, N_{bin}$; b) Re-sampling to obtain the bootstrap estimate of the error estimate: $\sigma_{\beta} = \sqrt{(N_{sample}^{(boot)} - 1)^{-1} \sum_{i=1}^{N_{sample}^{(boot)}} (\langle \beta \rangle_{(i)} - \langle \beta \rangle)^2}$. The only difference here is that $N_{bin} = 5$ since there is no crossing of seeds for this estimate.

So, our method follows the prescription:

1. We obtain two estimates of the dynamic exponent z (minimum and maximum) estimates where the error bars were obtained with bootstrap re-sampling, under $N_{sample}^{(boot)} = 10^4$.
2. From these two estimates (input), we obtain a list of worst and best estimates of the static exponent ν . From these estimates we select the nearest and the farthest estimates with uncertainties calculated by the bootstrap method.
3. Finally with best and worst values of ν , our re-sampling bootstrap results in a list of worst and best estimates of β and its uncertainty.

Interval	z	ν_{best}	ν_{worst}	β_{best}	β_{worst}
[70, 80]	2.28(5)	0.71(4)	0.66(4)	0.117(3)	0.104(3)
[80, 90]	2.25(5)	0.69(1)	0.64(1)	0.117(1)	0.104(1)
[90, 100]	2.35(4)	0.70(3)	0.65(2)	0.119(3)	0.106(3)
[100, 110]	2.36(7)	0.71(2)	0.66(2)	0.116(3)	0.103(3)
[110, 120]	2.32(6)	0.69(2)	0.64(2)	0.117(3)	0.104(3)
[120, 130]	2.32(6)	0.71(3)	0.66(3)	0.117(3)	0.104(2)
[130, 140]	2.30(3)	0.68(2)	0.63(2)	0.117(1)	0.104(1)
[140, 150]	2.27(4)	0.69(2)	0.64(2)	0.118(8)	0.105(3)

TABLE V: Results for the bootstrap by using the order parameter M_1

For example, for the order parameter M_1 we have the results for z according to 2nd column in TABLE V for the different intervals. Taking the two more different estimates (maximum and minimum) we replicated the bootstrap method in order to obtain candidate estimates for ν and β , which is shown in the columns 3, 4, 5, and last one in this same table. Here ν_{best} are the values

obtained for $z = 2.25$ while the values for ν_{worst} were obtained by using $z = 2.36$ as input. The columns β_{best} and β_{worst} correspond to the best and worst values by using previous input values. So we choice $\nu = 0.70(3)$ and $\beta = 0.119(3)$ as better estimates among best estimates. Similar analysis was performed for M_2 which is shown in 8th and 9th columns in TABLE IV of this manuscript.

Acknowledgements

R. da Silva was partly supported by the Brazilian Research Council CNPq. The authors thank CESUP (Super Computer Center of Federal University of Rio Grande do Sul) as well as Professor Leonardo G. Brunet (IF-UFRGS) for the available computational resources. We are grateful for support from Clustered Computing (ada.if.ufrgs.br). We also would like to thank for the anonymous referees of the Physical Review E for helpful suggestions.

* Electronic address: rdasilva@if.ufrgs.br
¹ L. Onsager, Phys. Rev. **65**, 117 (1944).
² J. M. Kosterlitz and D. J. Thouless, J. Phys. C **6**, 1181 (1973).
³ J. V. Jos , L. P. Kadanoff, S. Kirkpatrick, and D. R. Nelson, Phys. Rev. B **16**, 1217 (1977).
⁴ J. Cardy, J. Phys. A **13**, 1507 (1980), F. C. Alcaraz and R. Koberle, J. Phys. A **14**, 1169 (1981).
⁵ V. A. Fateev and A. B. Zamolodchikov, Phys. Lett. **92A**, 37 (1982).
⁶ F. C. Alcaraz, J. Phys. A **20**, 2511 (1987).
⁷ B. Bonnier, M. Hontebeyrie, and C. Meyers, Phys. Rev. B **39**, 4079 (1989).
⁸ R. J. Baxter, J. Phys. C **6**, L445 (1973).
⁹ M. den Nijs, Phys. Rev. B **31**, 266 (1985).
¹⁰ B. Bonnier and K. Rouidi, Phys. Rev. B **42**, 8157 (1990).
¹¹ B. Bonnier, and Y. Leroyer, Phys. Rev. B **44**, 9700 (1991).
¹² F. C. Alcaraz and A. L. Santos, Nucl. Phys. **B275**, 436 (1986).
¹³ B. Bonnier, Phys. Rev. B **44**, 390 (1991).
¹⁴ R. da Silva, N. Alves Jr., J. R. Drugowich de Fel cio, Phys. Rev. E **87**, 012131 (2013).
¹⁵ R. da Silva, H. A. Fernandes, J. R. Drugowich de Fel cio, W. Figueiredo, Comput. Phys. Commun. **184**, 2371 (2013).
¹⁶ R. da Silva, J. R. Drugowich de Fel cio, A. S. Martinez, Phys. Rev. E **85**, 066707 (2012).
¹⁷ K. S. Trivedi, Probability and Statistics with Realiability, Queuing, and Computer Science Applications, John Wiley and Sons Ltd., 2nd edition, Chichester, UK (2002).
¹⁸ L. Schulke, B. Zheng, Phys. Rev. E **62**, 7482 (2000).
¹⁹ K. Rouidi and Y. Leroyer, Phys. Rev. B **45**, 1013 (1992).
²⁰ W. H. Press, S. A. Teukolsky, W. T. Vetterling, B. P. Flannery, Numerical recipes in Fortran 77: the art of scientific computing, Cambridge University Press (1992).

²¹ C. Vanderzande, J. Phys. A: Math. Gen. **20**, L549 (1987).
²² R. H. Swendsen and J. S. Wang, Phys. Rev. Lett. **58**, 86 (1989).
²³ U. Wolff, Phys. Rev. Lett. **68**, 361 (1989).
²⁴ H. K. Janssen, B. Schaub, and B. Z. Schmittmann, Z. Physik. B **73**, 539 (1989).
²⁵ D. A. Huse, Phys. Rev. B **40**, 304 (1989).
²⁶ Z. B. Li, L. Schulke and B. Zheng, Phys. Rev. Lett. **74**, 3396 (1995).
²⁷ E. V. Albano, M. A. Bab, G. Baglietto, R.A. Borzi, T.S. Grigera, E.S. Loscar, D.E. Rodriguez, M.L. Rubio Puzzo, and G.P. Saracco, Rep. Prog. Phys. **74**, 02650 (2011).
²⁸ B. Zheng, Int. J. Mod. Phys. B **12** 1419 (1998).
²⁹ R. da Silva, N. A. Alves, and J. R. Drugowich de Fel cio, Phys. Lett. A **298**, 325 (2002).
³⁰ R. da Silva, N. A. Alves, J. R. Drugowich de Fel cio, Phys. Rev. E **66**, 026130 (2002).
³¹ R. da Silva, J. R. Drugowich de Fel cio, Phys. Lett. A, **333**, 277 (2004).
³² Here it is important to mention that the lattice was randomly vanished by considering only two spin variables, $n_i = 1$ and 2, differently of the experiments performed to calculate the critical exponents where the lattice was vanished by putting 1/5 of spin variables of each kind. Our choice was based on numerical experiments that showed to be appropriated for this kind of analysis. On the other hand, for the former prepared initial configurations, the exponent ζ probably does not correspond to the correct value $(d - 2\beta/\nu)/z$. However, this does not forbid our approach whereas in this stage of the paper, our aim was only to explore alternatives for the localization of the critical points and not to estimate critical exponents which was correctly performed in the appropriate section.